

Heterometallic Borole Complexes of Iron and Gold†

Pierre Braunstein,^{*,‡} Gerhard E. Herberich,^{*,§} Mark Neuschütz,^{‡,§}
Martin U. Schmidt,[§] Ulli Englert,[§] Pierre Lecante,^{||} and Alain Mosset^{||}

Laboratoire de Chimie de Coordination, UMR 7513 CNRS, Université Louis Pasteur,
67070 Strasbourg Cedex, France, Institut für Anorganische Chemie der Rheinisch
Westfälischen Technischen Hochschule Aachen, Prof. Pirlet Strasse 1, 52074 Aachen, Germany,
and Centre d'Elaboration de Matériaux et d'Etudes Structurales–CNRS,
29 Rue Jeanne Marvig, BP 4347, 31055 Toulouse Cedex 4, France

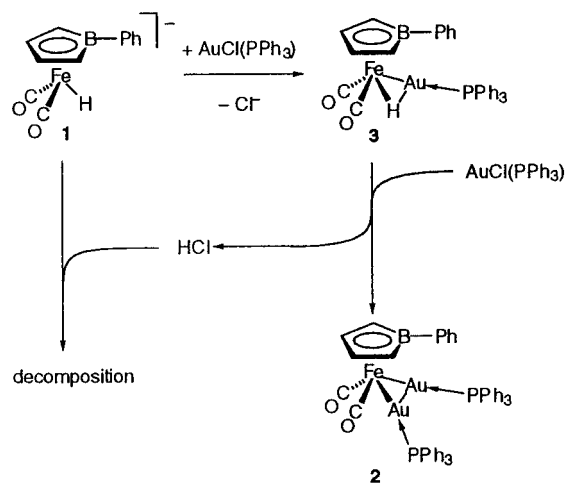
Received April 16, 1997

The first heterometallic borole complexes of Fe and Au have been prepared by reaction of $[\text{HFe}\{\eta^5\text{-}(1\text{-phenylborole})\}(\text{CO})_2]^-$ (**1**) with $[\text{AuCl}(\text{PPh}_3)]$ in CH_2Cl_2 , and the crystal structure of $[(\text{OC})_2\{\eta^5\text{-}(1\text{-phenylborole})\}\text{Fe}\{\text{Au}(\text{PPh}_3)\}_2]$ (**2**) reveals an interesting orientation of the borole ligand. This complex reacts with $[\text{AuCl}(\text{PPh}_3)]/\text{TIPF}_6$ in CH_2Cl_2 to give the new cationic FeAu_3 cluster $[(\text{OC})_2\{\eta^5\text{-}(1\text{-phenylborole})\}\text{Fe}\{\text{Au}(\text{PPh}_3)\}_3]\text{PF}_6$ (**4**) which has a tetrahedral metal core, as established by a wide angle X-ray scattering study.

Introduction

Organometallic complexes containing a direct metal–metal bond between gold (or silver or copper) and a transition metal carbonyl fragment have been among the first heterometallic complexes to be systematically investigated.¹ Their mode of preparation and structural relationship with the corresponding hydrido metal carbonyl complexes experimentally demonstrated the relationship between H^+ and $\text{Au}(\text{PR}_3)^+$ which became later the subject of numerous investigations performed in the context of the isolobal analogy.² Reaction of $[\text{Fe}(\text{CO})_4]^{2-}$ with 2 equiv of $[\text{AuCl}(\text{PPh}_3)]$ yielded the triangular complex $[(\text{OC})_4\text{Fe}\{\text{Au}(\text{PPh}_3)\}_2]$, which was the first mixed-metal gold cluster,^{1a} in which the Au–Au distance is 3.028 Å.^{3,4} The hydridometalate $[\text{HFe}(\text{CO})_3\{\text{P}(\text{OEt})_3\}]^-$ did not lead to the expected dinuclear Fe–Au complex, irrespective of the stoichiometry used between the iron and gold reagents. Instead, the FeAu_2 cluster $[(\text{OC})_3\{\text{EtO}\}_3\text{P}\{\text{Fe}\}\{\text{Au}(\text{PPh}_3)\}_2]$ was obtained, in which the Au–Au distance

Scheme 1. Formation of $[(\text{OC})_2\{\eta^5\text{-}(1\text{-Phenylborole})\}\text{Fe}\{\text{Au}(\text{PPh}_3)\}_2]$ (**2**) from **1**



is 2.872(2) Å.³ As part of our studies on the reactivity of borole-containing carbonylmetalates,⁵ we wondered whether the hydridometalate $[\text{HFe}\{\eta^5\text{-}(1\text{-phenylborole})\}(\text{CO})_2]^-$ (**1**), which is isoelectronic with $[\text{HFe}(\text{CO})_3\{\text{P}(\text{OEt})_3\}]^-$, would also readily lose its hydrido ligand (in the form of a proton) to give a cluster complex or whether isolation of an intermediate bimetallic Fe–Au hydrido complex could be possible.

Results and Discussion

Reactions of the hydridoferrate $[\text{HFe}\{\eta^5\text{-}(1\text{-phenylborole})\}(\text{CO})_2]^-$ (**1**)⁶ in CH_2Cl_2 with 0.5–4 equiv of $[\text{AuCl}(\text{PPh}_3)]$ afforded the iron–digold complex $[\{\eta^5\text{-}(1\text{-phenylborole})\}\text{Fe}(\text{CO})_2\{\text{Au}(\text{PPh}_3)\}_2]$ (**2**), which crystallized from acetone as yellow cubes. However, significant decomposition was observed that could be caused by the

(5) Braunstein, P.; Englert, U.; Herberich, G. E.; Neuschütz, M. *Angew. Chem., Int. Ed. Engl.* **1995**, *34*, 1010.

(6) Herberich, G. E.; Carstensen, T.; Klaff, N.; Neuschütz, M. *Chem. Ber.* **1992**, *125*, 1801.

† This work is based on the Ph.D. thesis of M.N.

‡ Université Louis Pasteur.

§ Rheinisch Westfälische Technische Hochschule Aachen.

|| Centre d'Elaboration de Matériaux et d'Etudes Structurales.

(1) (a) Coffey, C. E.; Lewis, J.; Nyholm, R. S. *J. Chem. Soc.* **1964**, 1741. (b) Kasenally, A. S.; Nyholm, R. S.; O'Brien, R. J.; Stiddard, M. H. B. *Nature* **1964**, *204*, 871. (c) Kasenally, A. S.; Nyholm, R. S.; Stiddard, M. H. B. *J. Am. Chem. Soc.* **1964**, *86*, 1884.

(2) (a) Lauher, J. W.; Wald, K. *J. Am. Chem. Soc.* **1981**, *103*, 7648. (b) Evans, D. G.; Mingos, D. M. P. *J. Organomet. Chem.* **1982**, *232*, 171. (c) Braunstein, P.; Lehner, H.; Matt, D.; Tiripicchio, A.; Tiripicchio Camellini, M. *Angew. Chem., Int. Ed. Engl.* **1984**, *23*, 304; *Angew. Chem.* **1984**, *96*, 307. (d) Hall, K. P.; Mingos, D. M. P. *Prog. Inorg. Chem.* **1984**, *32*, 237. (e) Braunstein, P.; Rosé, J. *Gold Bull.* **1985**, *18*, 17. (f) Mueting, A. M.; Bos, W.; Alexander, B. D.; Boyle, P. D.; Casalnuovo, J. A.; Balaban, S.; Ito, L. N.; Johnson, S. M.; Pignolet, L. H. *New J. Chem.* **1988**, *12*, 505. (g) Salter, I. D. *Adv. Organomet. Chem.* **1989**, *29*, 284. (h) Bruce, M. I.; Corbin, P. E.; Humphrey, P. A.; Koutsantonis, G. A.; Liddell, M. J.; Tiekink, E. R. T. *J. Chem. Soc., Chem. Commun.* **1990**, 674. (i) Salter, I. D. In *Comprehensive Organometallic Chemistry II*; Abel, E. W., Stone, F. G. A., Wilkinson, G., Eds.; Pergamon: New York, 1995, Vol. 10, pp 255–322.

(3) Arndt, L. W.; Ash, C. E.; Darensbourg, M. Y.; Hsiao, Y. M.; Kim, C. M.; Reibenspies, J.; Youngdahl, K. A. *J. Organomet. Chem.* **1990**, *394*, 733.

(4) Briant, C. E.; Hall, K. P.; Mingos, D. M. P. *J. Chem. Soc., Chem. Commun.* **1983**, 843.

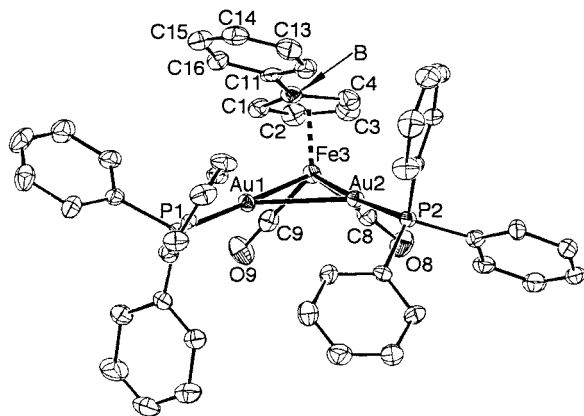


Figure 1. Displacement ellipsoid plot⁷ (30% probability) of [(OC)₂{ η^5 -(1-phenylborole)}Fe{Au(PPh₃)₂}₂] (**2**).

Table 1. Selected Interatomic Distances (Å) in [(η^5 -(1-Phenylborole))Fe(CO)₂(AuPPh₃)₂] (**2**)

Au1–Au2	2.737(1)	Fe3–B	2.29(1)
Au1–Fe3	2.567(1)	Fe3–C1	2.118(8)
Au1–P1	2.269(2)	Fe3–C2	2.059(9)
Au1–C9	2.667(9)	Fe3–C3	2.057(9)
Au1–B	3.06(1)	Fe3–C4	2.137(9)
Au2–Fe3	2.586(1)	C1–B	1.52(1)
Au2–P2	2.271(2)	C1–C2	1.43(1)
Au2–C8	2.609(9)	C2–C3	1.41(1)
Au2–B	3.30(1)	C3–C4	1.43(1)
Fe3–C8	1.749(9)	C4–B	1.54(1)
Fe3–C9	1.75(1)	B–C11	1.56(1)
O8–C8	1.16(1)		
O9–C9	1.16(1)		

HCl liberated during the formation of **2** (Scheme 1). Protonation of the hydridoferrate **1** has indeed been independently shown to lead to decomposition.⁶ The reaction is assumed to proceed via the hydrido-bridged bimetallic complex [(OC)₂{ η^5 -(1-phenylborole)}Fe(μ -H){Au(PPh₃)₂}] (**3**) (see below). Formal replacement of a hydride ligand by Au(PPh₃)⁺ was previously observed to readily lead to a digold–metal complex, as in the case of the first PtAu₂ cluster.^{2c}

The protons liberated on going from **3** to **2** may be trapped by triethylamine, thereby suppressing the side reactions and improving the yield of the iron–digold complex **2** to approximately 60%. Complex **2** has been characterized by ¹H, ¹¹B, ¹³C{¹H}, and ³¹P{¹H} NMR and infrared spectroscopy and by an X-ray diffraction study. A view of the molecular structure of **2** is shown in Figure 1, and selected interatomic distances and angles are reported in Tables 1 and 2.

In the crystal, compound **2** has no symmetry element although the three metals form a nearly isosceles triangle. The Fe–Au–P bond angles are less than 170°, as typically found in complexes containing a Ph₃P–Au–Au–PPh₃ unit.^{2c–1} The distance of 2.737(1) Å between the two gold atoms is significantly shorter than in related FeAu₂ complexes and in gold metal (2.884 Å)⁸ (Table 3).

There are two extreme ways of considering the bonding involving the two phosphine gold fragments in **2**, represented in Scheme 2. A description of the iron–

Table 2. Selected Bond Angles in [(η^5 -(1-Phenylborole))Fe(CO)₂(AuPPh₃)₂] (**2**) (deg)

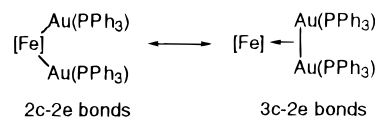
Au1–Au2–Fe3	57.58(3)	Au1–Fe3–C2	122.9(3)
Au2–Au1–Fe3	58.27(3)	Au1–Fe3–C3	145.5(3)
Au1–Fe3–Au2	64.15(3)	Au1–Fe3–C4	111.3(3)
Au1–Au2–B	59.9(2)	Au2–Fe3–B	85.1(3)
Au2–Au1–B	69.3(2)	Au2–Fe3–C1	122.8(3)
Au2–B–Au2	50.8(2)	Au2–Fe3–C2	147.0(3)
Au1–Fe3–C8	116.8(3)	Au2–Fe3–C3	113.6(3)
Au1–Fe3–C9	73.6(3)	Au2–Fe3–C4	80.4(3)
Au2–Fe3–C8	71.0(3)	C2–C1–B	110.0(9)
Au2–Fe3–C9	117.1(3)	C1–C2–C3	109.7(8)
C8–Fe3–C9	91.0(4)	C2–C3–C4	109.2(9)
Fe3–C8–O8	173.8(8)	C3–C4–B	109.7(9)
Fe3–C9–O9	175.8(8)	C1–B–C4	101.0(8)
Au1–Fe3–B	77.8(3)	Fe3–Au1–P1	168.71(6)
Au1–Au2–P2	133.15(5)	Fe3–Au2–P2	169.17(6)
Au1–Fe3–C1	84.7(3)	Au2–Au1–P1	132.35(5)

Table 3. Au–Au Distances in Compounds of the Type FeAu₂

compound	distance (Å)
[Fe](AuPPh ₃) ₂ (2) ^a	2.737(1)
[(OC) ₄ Fe(AuPPh ₃) ₂] ^{b–d}	3.028
[(EtO) ₃ P](OC) ₃ Fe(AuPPh ₃) ₂ ^c	2.872(2)
[(OC) ₄ Fe{Au(μ -dppf)Au} ₂ Fe(CO) ₄] ^d	2.977(1)

^a [Fe] stands for [η^5 -(1-phenylborole)]Fe(CO)₂, this work. ^b Reference 1a. ^c Reference 3. ^d Reference 4.

Scheme 2



gold interactions as 2c–2e bonds leads to a 18 VE iron complex with two terminal phosphine–gold groups, similar to the dihydrido iron complex [H₂Fe(CO)₄].^{2h,9} When a 3c–2e bonding system is considered, the Au₂ fragment serves as a σ -donor to the iron and its unoccupied σ^* orbital can accept back-bonding from the iron.² Strong back-donation from iron therefore leads to a lengthening of the gold–gold distance, making these two alternative descriptions structurally undistinguishable. The short gold–gold distance in **2** shows that the 3c–2e bond description represents an important contribution to the actual bonding. Simulation of the AA'XX'-type (A = A' = C, X = X' = P) resonances observed in the ¹³C{¹H} NMR spectrum for the ipso, ortho, meta, and para carbons of the PPh₃ ligands of **2** allowed the determination of the P–P coupling constant, ³⁺⁴J_{PP} = 15 Hz. We are not aware of other determinations of this coupling constant which could be used on a comparative basis to evaluate the gold–gold bonding interaction.

In the crystal structure, the phenyl substituent of the borole ligand is located between the phenyl groups of the phosphine ligands, somewhat blocking the 1-phenylborole ligand above the two phosphine ligands. As a result of steric interactions, the phenyl substituent of the borole ring is rotated about the B–C(11) axis by about 10°; the torsion angles C(1)–B–C(11)–C(16) and C(4)–B–C(11)–C(12) are of 8.3(1.6) and 12.5(1.6)°, respectively. This ligand orientation is preferred over that with the borole ligand rotated by ca. 180° which would place the phenyl substituent toward the sterically

(7) Spek, A. L. *Acta Crystallogr.* **1990**, A46, C34; PLATON-94; University of Utrecht: Utrecht, 1994.

(8) *International Tables for X-Ray Crystallography*; Macgillavry, C. H., Rieck, G. D., Lonsdale, K., Eds.; The Kynoch Press: Birmingham, U.K., 1968; Vol. 3, p 277.

(9) McNeill, E. A.; Scholer, F. R. *J. Am. Chem. Soc.* **1977**, 99, 6243.

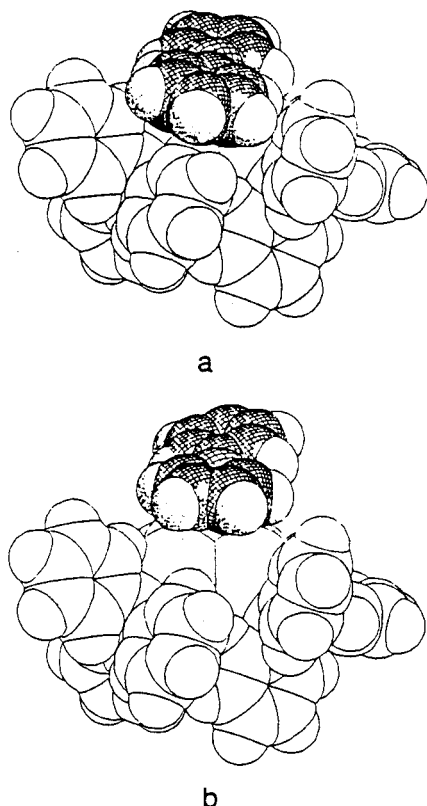


Figure 2. Space-filling views of the atropisomers of $[\{\eta^5\text{-}(1\text{-phenylborole})\}\text{Fe}(\text{CO})_2(\text{AuPPH}_3)_2]$ (**2**): (a) structure found; (b) borole ligand rotated by 180° .

less congested "outside" of the molecule (Figure 2) and could be due to boron–gold bonding interactions although the Au(1)–B and Au(2)–B distances of 3.06(1) and 3.30(1) Å, respectively, are rather long. For comparison, a Pd–B separation of 2.59(2) Å was observed in the planar, triangulated cluster $[\{\eta^5\text{-}(1\text{-phenylborole})\}\text{Re}(\text{CO})_3\text{Pd}]_2$.⁵ Rather short contacts are observed between the gold atoms Au(1) and C(9) (2.667(9) Å) and Au(2) and C(8) (2.609(9) Å), which suggests some semibridging character for these carbonyl ligands and is consistent with their slight bending (Figure 3). A comparable Au–C contact of 2.60 Å has been found in $[(\text{OC})_3\{\text{EtO}\}_3\text{P}\}\text{Fe}\{\text{Au}(\text{PPh}_3)\}_2$.³ However, nonbonding contacts of this type have been observed previously and these distances should therefore be interpreted with caution.¹⁰

In order to find out whether the phenyl group of the borole ligand has to be preoriented during the synthesis of the FeAu₂ cluster before adopting the conformation found in the solid state or becomes "locked" between the phosphine ligands as a result of subsequent rearrangement in the cluster, a NOE experiment was performed on complex **2**. Irradiation with the resonance frequency of the ortho protons of the phosphine phenyls led to a difference spectrum which showed a positive effect for the 2,5 and 3,4 borole protons (ratio 2:1). The stronger signal for the 2,5 protons is not unexpected as they are closer to the ortho protons of the phosphine phenyls in the ground state conformation of the molecule than the 3,4 borole protons. Since it is difficult to quantitatively

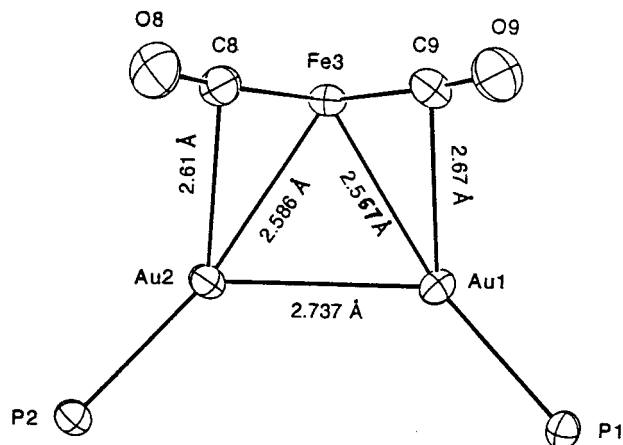
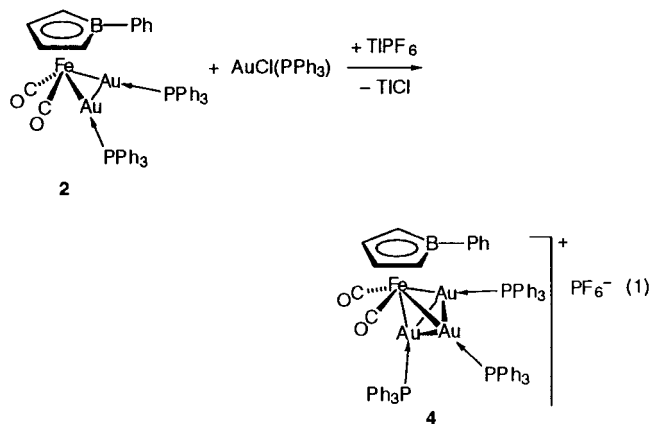


Figure 3. ORTEP plot of the fragment $(\text{OC})_2\text{Fe}(\text{AuPPH}_3)_2$ of $[\{\eta^5\text{-}(1\text{-phenylborole})\}\text{Fe}(\text{CO})_2(\text{AuPPH}_3)_2]$ (**2**) (iron and gold atoms in the projection plane).

interpret the NOE in terms of distances or probability of a given conformation, this result simply does not contradict the possibility of a dynamic situation once the complex is formed, which would allow the borole ligand to rotate, for example by opening of the Au–Au bond.¹¹

We then examined the reaction of the FeAu₂ cluster **2** with $[\text{AuCl}(\text{PPh}_3)]/\text{TIPF}_6$ in CH_2Cl_2 , which afforded the new cationic FeAu₃ cluster $[(\text{OC})_2\{\eta^5\text{-}(1\text{-phenylborole})\}\text{Fe}\{\text{Au}(\text{PPh}_3)\}_3]\text{PF}_6$ (**4**) as the only product (eq 1). This tetranuclear cluster has been characterized by



^1H , $^{13}\text{C}\{^1\text{H}\}$, $^{31}\text{P}\{^1\text{H}\}$ NMR, and IR spectroscopy. Since the compound has shown no tendency to form single crystals suitable for X-ray diffraction and a powder sample proved to be amorphous, a wide angle X-ray scattering (WAXS) study on the amorphous material was carried out which established the tetrahedral structure of the cluster. The WAXS technique is known to provide information about short and medium-range order in noncrystalline samples.¹² It has been successfully applied to the study of inorganic glasses,¹³ nanocrystalline particles,¹⁴ and amorphous molecular sol-

(10) Braunstein, P.; Rosé, J.; Dedieu, A.; Dusausoy, Y.; Mangeot, J.-P.; Tiripicchio, A.; Tiripicchio-Camellini, M. *J. Chem. Soc., Dalton Trans.* **1986**, 225.

(11) Another way to elucidate this question could be the use of a bridging diphosphine ligand to strengthen the Au–Au bond, although experiments by Mingos *et al.* describe condensation of two FeAu₂ units by diphosphines as dppm or dppe.⁴

(12) Warren, B. E. *X-Ray Diffraction*; Dover Publications: New York, 1990.

(13) Burian, A.; Lecante, P.; Mosset, A.; Galy, J. Z. *Kristallogr.* **1990**, *193*, 199.

Infrared spectra were recorded on FT-IR Perkin-Elmer 1720 X and FT-IR Bruker IFS66/113 spectrometers. NMR spectra were recorded on Varian VXR 500 (^1H , 500 MHz, relative to TMS; ^{13}C , 125.70 MHz, relative to TMS; ^{31}P , 202.33 MHz, relative to H_3PO_4), Bruker SY 200 (^1H , 200 MHz, relative to TMS), and Bruker WP 80 SY (^1H , 80 MHz, relative to TMS) spectrometers. The mass spectrum was obtained with a FAB Fisons ZAB-HF spectrometer. The elemental analyses were performed by the Analytisches Labor Pascher (Remagen, Germany). The hydridoferrate complex **1** was obtained from $[\{\eta^5\text{-}(1\text{-phenylborole})\}\text{Fe}(\text{CO})_3]$ using the Hieber's base reaction,⁶ and the gold complex $[\text{AuCl}(\text{PPh}_3)]$ was prepared by treating tetrachloroauric acid with 2 equiv of PPh_3 .²⁴

Preparation of $[\eta^5\text{-}(1\text{-Phenylborole})\text{Fe}(\text{CO})_2\{\text{Au}(\text{PPh}_3)_2\}]$ (2**).** Triethylamine (4 drops) was added to a solution of $\text{Bu}_4\text{N}[\text{HfE}\{\eta^5\text{-}(1\text{-phenylborole})\}(\text{CO})_2]$ (**1**) (145 mg, 0.29 mmol) in acetone (3 mL). Solid $[\text{AuCl}(\text{PPh}_3)]$ (290 mg, 0.58 mmol) was then added to this solution. The deep red color of the solution changed to dark brown, and a light solid precipitated. The solid was filtered off, dried, and dissolved in a small amount of CH_2Cl_2 . This solution was purified by chromatography over a short column of silica gel 60. Evaporation of the solvent *in vacuo* and crystallization from acetone yielded $[\{\eta^5\text{-}(1\text{-phenylborole})\}\text{Fe}(\text{CO})_2\{\text{Au}(\text{PPh}_3)_2\}]$ (**2**) (217 mg, 0.19 mmol, 64%) as yellow cubes. Anal. Calcd for $\text{C}_{48}\text{H}_{39}\text{Au}_2\text{BF}_6\text{O}_2\text{P}_2$: C, 49.26; H, 3.36. Found: C, 49.12; H, 2.96. IR: (THF) $\nu(\text{CO})$ 1935 (s), 1886 (s) cm^{-1} ; (KBr) $\nu(\text{CO})$ 1929 (s), 1881 (s) cm^{-1} . ^1H NMR: (200 MHz, d_6 -acetone) δ 7.15 (m, 35 H, phenyl), 5.02 (m, 2 H, $N=6$ Hz, 3,4-borole), 3.96 (m, 2H, $N=6$ Hz, 2,5-borole); (500 MHz, CD_2Cl_2) δ 7.41, 6.91, 6.80 (m, 35H, phenyl), 5.07 (m, 2H, $N=5.8$ Hz, 3,4-borole), 3.98 (m, 2H, $N=5.8$ Hz, 2,5-borole). $^{11}\text{B}\{^1\text{H}\}$ NMR (160 MHz, CD_2Cl_2): δ 15.2 (s br, 1 B). $^{13}\text{C}\{^1\text{H}\}$ NMR (126 MHz, CD_2Cl_2): δ 219.26 (s, 2C, CO), 141.6 (s br, 1C, *ipso*-phenylborole), 134.96 (s, 2C, *ortho*-phenylborole), 134.40 (m, 12C, $^2J_{\text{CP}} = 15.3$ Hz, $^{5+6}J_{\text{CP}} = -1$ Hz, $^{3+4}J_{\text{PP}} = 15$ Hz, *ortho*-phenylphosphine), 132.01 (m, 6C, $^1J_{\text{CP}} = 49.6$ Hz, $^{4+5}J_{\text{CP}} = -3$ Hz, $^{3+4}J_{\text{PP}} = 15$ Hz, *ipso*-phenylphosphine), 131.10 (s, 6C, *para*-phenylphosphine), 129.22 (m, 12C, $^3J_{\text{CP}} = 11.4$ Hz, $^{6+7}J_{\text{CP}} = -1$ Hz, $^{3+4}J_{\text{PP}} = 15$ Hz, *meta*-phenylphosphine), 127.33 (s, 2C, *meta*-phenylborole), 126.55 (s, 1C, *para*-phenylborole), 85.14 (s, 2C, 3,4-borole), 72.19 (s (br), 2C, 2,5-borole). Coupling constants were determined by spectral simulation. $^{31}\text{P}\{^1\text{H}\}$ NMR (202 MHz, CD_2Cl_2): δ 40.29 (s, 2P). MS (FAB⁺, NBA): sample decomposes to $[\{\eta^5\text{-}(1\text{-phenylborole})\}\text{Fe}(\text{CO})_2\{\text{Au}(\text{PPh}_3)_3\}]^+$.

Preparation of $[\{\eta^5\text{-}(1\text{-Phenylborole})\}\text{Fe}(\text{CO})_2\{\text{Au}(\text{PPh}_3)_3\}]\text{PF}_6$ (4**).** The reaction of 1 equiv of **1** with 3 equiv each of $[\text{AuCl}(\text{PPh}_3)]$ and TIPF_6 in CH_2Cl_2 afforded an orange solution. It was filtered, and crystallization afforded $[\{\eta^5\text{-}(1\text{-phenylborole})\}\text{Fe}(\text{CO})_2\{\text{Au}(\text{PPh}_3)_3\}]\text{PF}_6$ (**4**) as the only product. Alternatively, the reaction of **2** with $[\text{AuCl}(\text{PPh}_3)]$ and TIPF_6 (1:1:1 ratio) in CH_2Cl_2 afforded the same product. Attempts to obtain single crystals of **4** failed. An orange solid was obtained and shown to be spectroscopically pure. Anal. Calcd for $\text{C}_{66}\text{H}_{44}\text{Au}_3\text{BF}_6\text{FeO}_2\text{P}_4$: C, 44.93; H, 2.51. Found: C, 44.42; H, 2.46. IR: (CH_2Cl_2) $\nu(\text{CO})$ 1977 (s), 1934 (s) cm^{-1} ; (KBr) $\nu(\text{CO})$ 1969 (s), 1925 (s) cm^{-1} . ^1H NMR: (200 MHz, d_6 -acetone) δ 7.45, 6.64 (m, 50H, phenyl), 5.70 (m, 2H, $N=6$ Hz, 3,4-borole), 4.47 (m, 2H, $N=6$ Hz, 2,5-borole); (500 MHz, CD_2Cl_2) δ 7.2 (m, 50H, phenyl), 5.51 (m, 2H, 3,4-borole), 4.29 (m, 2H, 2,5-borole). $^{13}\text{C}\{^1\text{H}\}$ NMR (126 MHz, CD_2Cl_2) δ 136.40 (s, 2C, *ortho*-phenylborole), 134.18 (m, 18C, *ortho*-phenylphosphine), 132.14 (s, 9C, *para*-phenylphosphine), 130.35 (s, 2C, *meta*-phenylborole), 129.74 (m, 18C, *meta*-phenylphosphine), 128.20 (s, 1C, *para*-phenylborole), 89.74 (s, 2C, 3,4-borole). $^{31}\text{P}\{^1\text{H}\}$ NMR (202 MHz, CD_2Cl_2): δ 44.71 (s, 3P).

Reaction of $[\{\eta^5\text{-}(1\text{-Phenylborole})\}\text{Fe}(\text{CO})_2\{\text{Au}(\text{PPh}_3)_2\}]$ (2**) with Trifluoroacetic Acid.** Since the hydrido-bridged

Table 5. Crystallographic Data, Data Collection Parameters, and Refinement Results for 2

empirical formula	$\text{C}_{48}\text{H}_{39}\text{Au}_2\text{BF}_6\text{O}_2\text{P}_2$
fw	1170.38
cryst syst	monoclinic
space group	$P2_1/c$ (No. 14)
<i>a</i> , Å	20.863(8)
<i>b</i> , Å	11.321(6)
<i>c</i> , Å	20.64(1)
β , deg	119.56(4)
<i>U</i> , Å ³	4241(8)
<i>d</i> _{calc} , g cm ⁻³	1.833
<i>Z</i>	4
<i>F</i> (000), electrons	2248
μ , cm ⁻¹	73.39
radiation (λ , Å)	Mo K α (0.7107)
<i>T</i> , K	258
scan mode (θ range, deg)	ω (3–27)
no. of total data	9882
no. of unique data	8807
no. of unique obsd data	6339 ($I > \sigma(I)$)
no. of variables	505
<i>R</i> , <i>R</i> _w ^a	0.045, 0.040
max resid dens, e Å ⁻³	0.8 between Au1 and Fe

$$^a R = \sum ||F_o| - |F_c|| / \sum |F_o|. R_w = [\sum w(|F_o| - |F_c|)^2 / \sum w|F_o|^2]^{1/2}. w^{-1} = \sigma^2(F_o).$$

complex $[\{\eta^5\text{-}(1\text{-phenylborole})\}\text{Fe}(\text{CO})_2(\mu\text{-H})\{\text{Au}(\text{PPh}_3)\}]$ (**3**) could not be isolated analytically pure owing to its lability, this reaction was carried out in an NMR tube. The quantities were chosen to guarantee a default of trifluoroacetic acid. To a solution of **2** (93 mg, 0.08 mmol) in CD_2Cl_2 (approximately 0.5 mL) in a 5 mm NMR tube was added trifluoroacetic acid (approximately 1 μL , 0.01 mmol) with a microsyringe. The ^1H NMR spectrum showed the presence of **2** (73%), of the cationic cluster **4** (13.5%), and of $[\{\eta^5\text{-}(1\text{-phenylborole})\}\text{Fe}(\text{CO})_2(\mu\text{-H})\{\text{Au}(\text{PPh}_3)\}]$ (**3**) (13.5%). Integration of the $^{31}\text{P}\{^1\text{H}\}$ NMR signals gave a ratio of 72.8% for the FeAu_2 cluster **2**, 20.4% for **4**, and 6.8% for **3**. Spectroscopic data for $[\{\eta^5\text{-}(1\text{-phenylborole})\}\text{Fe}(\text{CO})_2(\mu\text{-H})\{\text{Au}(\text{PPh}_3)\}]$ (**3**): IR, (CH_2Cl_2) $\nu(\text{CO})$ 1989 (s), 1932 (s) cm^{-1} ; (THF) $\nu(\text{CO})$ 1988 (s), 1932 (s) cm^{-1} . ^1H NMR (80 MHz, CD_2Cl_2): δ 5.27 (m, 2H, partly masked by the solvent signal, 3,4-borole), 3.62 (m, 2H, 2,5-borole), -9.42 (d, 1H, $^2J_{\text{HP}} = 79$ Hz, hydride). ^{31}P NMR (202 MHz, CD_2Cl_2 , protons with chemical shifts between 0 and 10 ppm decoupled): δ 47.13 (d, 1 P, $^2J_{\text{HP}} = 77$ Hz).

X-ray Structure Determination of 2. The data collection was performed on an ENRAF-Nonius CAD4 diffractometer with Mo K α radiation (graphite monochromator). Crystal data, data collection parameters, and refinement results are given in Table 5. An empirical absorption correction on the basis of azimuthal scans²⁵ (minimum transmission 0.861, maximum transmission 1.000) was applied to the data set before symmetry-related reflections were merged. The structure was solved by conventional heavy atom methods followed by Fourier difference syntheses and refined on structure factors with the SDP program system.²⁶ All non-hydrogen atoms were refined with anisotropic displacement parameters, whereas hydrogen atoms were treated as riding on their carbon atoms. Refinement converged for 505 parameters using a statistical weighting scheme $w = 1/[\sigma^2(F_o)]$ at values of $R = 0.045$ and $R_w = 0.040$ with a goodness of fit of 1.095.²⁷

WAXS Experiment with 4. WAXS measurements were performed in transmission mode on a CAD-4 ENRAF-NONIUS

(25) North, A. C. T.; Phillips, D. C.; Mathews, F. S. *Acta Crystallogr.* **1968**, *A24*, 351.

(26) SDP, version 5.0; ENRAF-Nonius: Delft, The Netherlands, 1989.

(27) Further details of the crystal structure analyses are available on request from the Fachinformationszentrum Karlsruhe, Gesellschaft für wissenschaftlich-technische Information mbH, D-76344 Eggenstein-Leopoldshafen, Germany, on quoting the depository number CSD-408517.

(24) (a) Hass, A.; Helmbrecht, J.; Niemann, U. In *Handbuch der Präparativen Anorganischen Chemie*; Brauer, G., Ed.; Ferdinand Enke Verlag: Stuttgart, 1978; Vol. 2, pp 971–1021. (b) Braunstein, P.; Lehner, H.; Matt, D. *Inorg. Synth.* **1990**, *27*, 218–221.

diffractometer using graphite-monochromatized Mo K α radiation ($\lambda = 0.7107 \text{ \AA}$). The sample was prepared by pelleting a small amount of the pure compound. Because of the strong fluorescence radiation from gold atoms, a zirconium attenuator was set between the sample and the detector. A second measurement without the attenuator was also performed in order to extract a fluorescence profile for further correction. All data sets included 459 points equally spaced in s ($s = 4\pi \sin \theta/\lambda$) on a θ range extending from 1.5 to 70°. Data were corrected for air scattering, fluorescence, absorption, and polarization using procedures previously described.²⁸ After normalization using the methods of Norman²⁹ and Krogh-Moe,³⁰ the so-called reduced intensity $i(s)$ was extracted. A Fourier transform of $i(s)$ provided a reduced radial distribution function (RDF) whose maxima can be related to interatomic distances within the sample. The Debye formula^{12,31} was used to calculate scattering intensities for a number of different models for the cation with tetrahedral, planar, and butterfly-type arrangements of the metal atoms. Only the tetrahedral

model is able to fit the RDF in the distance range below ca. 6 Å. The model used for the calculated RDF in Figure 4 was based on the following assumptions: the metal core was taken as an almost regular tetrahedron (Au–Au = 2.70 Å, Au–Fe = 2.74 Å), with a triphenylphosphane ligand bonded to each gold atom (Au–P = 2.25 Å). The (phenylborole)Fe(CO)₂ moiety was oriented such that the carbonyl groups exhibit Au–C distances of 2.60 Å.

Acknowledgment. We are grateful to the DAAD for a grant to M.N., the Centre National de la Recherche Scientifique (Paris) for financial support, and Johnson Matthey PLC for a generous loan of HAuCl₄.

Supporting Information Available: Tables of atomic coordinates for the non-hydrogen atoms (Table S-I), atomic coordinates for the hydrogen atoms (Table S-II), anisotropic displacement parameters for the non-hydrogen atoms (Table S-III), and complete lists of bond distances and angles (Table S-IV) (13 pages). Ordering information is given on any current masthead page.

OM9703189

(28) Lecante, P.; Mosset, A.; Galy, J. *J. Mater. Sci.* **1992**, *27*, 3286.

(29) Norman, N. *Acta Crystallogr.* **1957**, *10*, 370.

(30) Krogh-Moe, J. *Acta Crystallogr.* **1956**, *9*, 951.

(31) Debye, P. *Ann. Phys. (Leipzig)* **1915**, *46*, 809.